Original article

Meshless method based on RBFs for solving three-dimensional multi-term time fractional PDEs arising in engineering phenomenons

Fuzhang Wang [a,b,c], Imtiaz Ahmad [d,*], Hijaz Ahmad [e,f], M.D. Alsulami [g], K.S. Alimgeer [h,*], Clemente Cesarano [e], Taher A. Nofal [i]

[a] Nanchang Institute of Technology, Nanchang 330044, China
[b] College of Computer Science and Technology, Huaibei Normal University, 235000 Huaibei, China
[c] School of Mathematical and Statistics, Xuzhou University of Technology, Xuzhou 221018, Jiangsu, China
[d] Department of Mathematics, University of Swabi, Khyber Pakhtunkhwa, Pakistan
[e] Section of Mathematics, International Telematic University Uninettuno, Corso Vittorio Emanuele II, 39, 00186 Roma, Italy
[f] Mathematics in applied sciences and engineering research group, Scientific Research Center, Al-Ayen University, Thi-Qar, 64001, Iraq
[g] University of Jeddah, College of Sciences and Arts at Alkamil, Department of Mathematics, Jeddah, Saudi Arabia
[h] Department of Electrical and Computer Engineering, COMSATS University, Islamabad Campus, Islamabad, Pakistan
[i] Department of Mathematics, College of Science, Taif University, P.O. Box 11099, Taif 21944, Saudi Arabia

A R T I C L E   I N F O

A B S T R A C T

The applications of fractional partial differential equations (PDEs) in diverse disciplines of science and technology have caught the attention of many researchers. This article concerned with the approximate numerical solutions of three-dimensional two- and three-term time fractional PDE models utilizing an accurate, and computationally attractive local meshless technique. Due to their tremendous advantages like ease of applicability in higher dimensions in both regular and irregular domains, the interest in meshless techniques is increasing. Test problems are considered to assess the reliability and accuracy of the proposed technique.

1. Introduction

Fractional PDE models are widely employed in many disciplines of physics, and variety of methods are used in the literature for their simulations (see Ain and He, 2019; Nadeem and Li, 2019; He and El-Dib, 2020a). Nowadays, it is in the limelight of active researchers with extensive research to advance numerical and analytical solutions for linear and nonlinear fractional PDEs (He and El-Dib, 2020b; He and Ain, 2020; He et al., 2012; Ahmad et al., 2018, 2020a,b,c; Srivastava et al., 2020; He, 2018; Inc et al., 2020; He, 2014). In the current work, we have considered the following two- and three-term time fractional Sobolev equation

$$\frac{\partial^{\gamma_1}\mathscr{U}(\overline{\mathbf{x}},t)}{\partial t^{\gamma_1}} + \frac{\partial^{\gamma_2}\mathscr{U}(\overline{\mathbf{x}},t)}{\partial t^{\gamma_2}} - \frac{\partial \nabla^2 \mathscr{U}(\overline{\mathbf{x}},t)}{\partial t} - \beta \nabla^2 \mathscr{U}(\overline{\mathbf{x}},t)$$
$$+ \gamma \nabla(\mathscr{U}(\overline{\mathbf{x}},t)\nabla \mathscr{U}(\overline{\mathbf{x}},t)) + \delta \mathscr{U}(\overline{\mathbf{x}},t) = F(\overline{\mathbf{x}},t), \quad \overline{\mathbf{x}} = (x,y,z) \in \Omega,$$
$$0 < \gamma_2 \leqslant \gamma_1 \leqslant 1, \, t > 0, \tag{1}$$

$$\frac{\partial^{\gamma_1}\mathscr{U}(\overline{\mathbf{x}},t)}{\partial t^{\gamma_1}} + \frac{\partial^{\gamma_2}\mathscr{U}(\overline{\mathbf{x}},t)}{\partial t^{\gamma_2}} + \frac{\partial^{\gamma_3}\mathscr{U}(\overline{\mathbf{x}},t)}{\partial t^{\gamma_3}} - \frac{\partial \nabla^2 \mathscr{U}(\overline{\mathbf{x}},t)}{\partial t} - \beta \nabla^2 \mathscr{U}(\overline{\mathbf{x}},t)$$
$$+ \gamma \nabla(\mathscr{U}(\overline{\mathbf{x}},t)\nabla \mathscr{U}(\overline{\mathbf{x}},t)) + \delta \mathscr{U}(\overline{\mathbf{x}},t) = F(\overline{\mathbf{x}},t), \quad \overline{\mathbf{x}} = (x,y,z) \in \Omega,$$
$$0 < \gamma_3 \leqslant \gamma_2 \leqslant \gamma_1 \leqslant 1, \, t > 0, \tag{2}$$

with conditions

$$\mathscr{U}(\overline{\mathbf{x}},0) = \mathscr{U}_0(\overline{\mathbf{x}}), \tag{3}$$

$$\mathscr{U}(\overline{\mathbf{x}},t) = g_1(\overline{\mathbf{x}},t), \quad \overline{\mathbf{x}} = (x,y,z) \in \partial\Omega, \tag{4}$$

where ∇^2 is the Laplacian and ∇ denote Gradient operators and β, γ, δ are known parameters whereas $\frac{\partial^{\gamma_1}}{\partial t^{\gamma_1}}, \frac{\partial^{\gamma_2}}{\partial t^{\gamma_2}}$ and $\frac{\partial^{\gamma_3}}{\partial t^{\gamma_3}}$ represent

* Corresponding authors.
E-mail addresses: imtiazkakakhil@gmail.com (I. Ahmad), hijaz555@gmail.com (H. Ahmad), saleem.khurram@gmail.com (K.S. Alimgeer).

the Caputo derivative operator of order $0 < \gamma_3 \leqslant \gamma_2 \leqslant \gamma_1 \leqslant 1$ for the function $\mathscr{U}(\overline{\mathbf{x}}, t)$.

Recent literature uses several meshless techniques to solve numerically different PDE models in almost all disciplines of physics and mathematics. In particular, the meshless techniques using radial basis function (RBF) are the main one of these processes. The meshless property makes it popular among researchers. These methods overcome the challenges of dimensionality using conventional methods. In contrast to mesh-based methods, meshless approaches do not need mesh in the domain. These techniques can compute the solution utilizing uniform or non-uniform nodes in both regular and irregular computational domains, which increases the applicability and usefulness of the methods. Meshless methods are in fact actionable and valuable that can be applied to solve physical problems (Wang et al., 2021; Hussain et al., 2020; Khan et al., 2020; Ahmad et al., 2019a, 2020d,e,f,g; Wang et al., 2019, 2020; Nawaz et al., 2021; Wang and Zheng, 2016).

Like other numerical methods, the meshless methods, have some drawbacks, which may be the most important one to choose the optimal value of the shape-parameter and dense ill-conditioned matrices. To circumvent these shortcomings, the local meshless technique is the best alternative proposed by researchers which is precise and stable in finding solutions for various integer and fractional PDE models (Ahmad et al., 2019b,c). These methods produce well conditioned sparse matrices and are less sensitive to the selection of shape-parameters than the global version. In addition, the local meshless method is extra valuable and effective than its global counterpart. Recently, these methods are explored in various form in different applications (Ahmad et al., 2017, 2020h; Shu, 2000).

In this paper, the local meshless technique is utilized for the solution of model Eqs. (1), (2). Inverse multiquadric (IMQ) radial basis functions (RBFs) are taken into account. Moreover, Two kinds of irregular domains are analyzed in numerical examinations.

2. Implementation of local meshless technique

According to the suggested technique, to approximated the derivatives of $\mathscr{U}(\overline{\mathbf{x}}, t)$ at the centers $\overline{\mathbf{x}}_h$ by the neighborhood of $\overline{\mathbf{x}}_h, \{\overline{\mathbf{x}}_{h1}, \overline{\mathbf{x}}_{h2}, \overline{\mathbf{x}}_{h3}, \ldots, \overline{\mathbf{x}}_{hn_h}\} \subset \{\overline{\mathbf{x}}_1, \overline{\mathbf{x}}_2, \ldots, \overline{\mathbf{x}}_{N^n}\}, n_h \ll N^n$, where $h = 1, 2, \ldots, N^n$. We have used $\overline{\mathbf{x}} = x, \overline{\mathbf{x}} = (x, y)$ and $\overline{\mathbf{x}} = (x, y, z)$ for one-, two- and three-dimensional cases respectively.

Procedure for one-dimensional case is

$$\mathscr{U}^{(m)}(x_h) \approx \sum_{k=1}^{n_h} \lambda_k^{(m)} \mathscr{U}(x_{hk}), h = 1, 2, \ldots, N. \tag{5}$$

Substituting the IMQ-RBF $\psi(\|y - y_p\|) = \frac{1}{\sqrt{1 + (c\|y_{hk} - y_p\|)^2}}$ in (5)

$$\psi^{(m)}(\|x_h - x_p\|) = \sum_{k=1}^{n_h} \lambda_{hk}^{(m)} \psi(\|x_{hk} - x_p\|), p = h1, h2, \ldots, hn_h. \tag{6}$$

Matrix form of (6)

$$\underbrace{\begin{bmatrix} \psi_{h1}^{(m)}(x_h) \\ \psi_{h2}^{(m)}(x_h) \\ \vdots \\ \psi_{hn_h}^{(m)}(x_h) \end{bmatrix}}_{\psi_{n_h}^{(m)}} = \underbrace{\begin{bmatrix} \psi_{h1}(x_{h1}) & \psi_{h2}(x_{h1}) & \cdots & \psi_{hn_h}(x_{h1}) \\ \psi_{h1}(x_{h2}) & \psi_{h2}(x_{h2}) & \cdots & \psi_{hn_h}(x_{h2}) \\ \vdots & \vdots & \ddots & \vdots \\ \psi_{h1}(x_{hn_h}) & \psi_{h2}(x_{hn_h}) & \cdots & \psi_{hn_h}(x_{hn_h}) \end{bmatrix}}_{\mathbf{A_{n_h}}} \underbrace{\begin{bmatrix} \lambda_{h1}^{(m)} \\ \lambda_{h2}^{(m)} \\ \vdots \\ \lambda_{hn_h}^{(m)} \end{bmatrix}}_{\lambda_{n_h}^{(m)}},$$

$$\tag{7}$$

where

$$\psi_p(x_k) = \psi(\|x_k - x_p\|), p = h1, h2, \ldots, hn_h,$$

for each $k = i1, h2, \ldots, hn_h$. (7) can be written as

$$\psi_{n_h}^{(m)} = \mathbf{A}_{n_h} \lambda_{n_h}^{(m)}, \tag{8}$$

From (8), we obtain

$$\lambda_{n_h}^{(m)} = \mathbf{A}_{n_h}^{-1} \psi_{n_h}^{(m)}. \tag{9}$$

(5) and (9) implies

$$\mathscr{U}^{(m)}(x_h) = \left(\lambda_{n_h}^{(m)}\right)^T \mathbf{V}_{n_h},$$

where

$$\mathbf{U}_{n_h} = \left[\mathscr{U}(x_{h1}), \mathscr{U}(x_{h2}), \ldots, \mathscr{U}(x_{hn_h})\right]^T.$$

The derivatives of $\mathscr{U}(x, y, t)$ w.r.t. x and y can be found as

$$\mathscr{U}_x^{(m)}(x_h, y_h) \approx \sum_{k=1}^{n_h} \gamma_k^{(m)} \mathscr{U}(x_{hk}, y_{hk}), h = 1, 2, \ldots, N^2,$$

$$\mathscr{U}_y^{(m)}(x_h, y_h) \approx \sum_{k=1}^{n_h} \eta_k^{(m)} \mathscr{U}(x_{hk}, y_{hk}), h = 1, 2, \ldots, N^2.$$

For $\gamma_k^{(m)}$ and $\eta_k^{(m)}$ $(k = 1, 2, \ldots, n_h)$, we continue as

$$\gamma_{n_h}^{(m)} = \mathbf{A}_{n_h}^{-1} \mathbf{\Phi}_{n_h}^{(m)},$$

$$\eta_{n_h}^{(m)} = \mathbf{A}_{n_h}^{-1} \mathbf{\Phi}_{n_h}^{(m)}.$$

Caputo derivative (Caputo, 1967) for $\gamma_1 \in (0, 1)$ is utilized for time derivative $\frac{\partial^{\gamma_1} \mathscr{U}(\overline{\mathbf{x}}, t)}{\partial t^{\gamma_1}}$ as follows

$$\frac{\partial^{\gamma_1} \mathscr{U}(\overline{\mathbf{x}}, t)}{\partial t^{\gamma_1}} = \begin{cases} \frac{1}{\Gamma(1-\gamma_1)} \int_0^t \frac{\partial \mathscr{U}(\overline{\mathbf{x}}, \vartheta)}{\partial \vartheta} (t - \vartheta)^{-\gamma_1} d\vartheta, & 0 < \gamma_1 < 1 \\ \frac{\partial \mathscr{U}(\overline{\mathbf{x}}, t)}{\partial t}, & \gamma_1 = 1. \end{cases}$$

To compute the derivative term we can proceed as follows, where $t_q = q\tau, q = 0, 1, 2, \ldots, Q$ and time step size $\Delta\tau$ in $[0, t]$.

$$\frac{\partial^{\gamma_1} \mathscr{U}(\overline{\mathbf{x}}, t_{q+1})}{\partial t^{\gamma_1}} = \frac{1}{\Gamma(1-\gamma_1)} \int_0^{t_{q+1}} \frac{\partial \mathscr{U}(\overline{\mathbf{x}}, \vartheta)}{\partial \vartheta} (t_{q+1} - \vartheta)^{-\gamma_1} d\vartheta,$$

$$= \frac{1}{\Gamma(1-\gamma_1)} \sum_{r=0}^{q} \int_{r\Delta\tau}^{(r+1)\Delta\tau} \frac{\partial \mathscr{U}(\overline{\mathbf{x}}, \vartheta)}{\partial \vartheta} (t_{r+1} - \vartheta)^{-\gamma_1} d\vartheta,$$

$$\approx \frac{1}{\Gamma(1-\gamma_1)} \sum_{r=0}^{q} \int_{r\Delta\tau}^{(r+1)\Delta\tau} \frac{\partial \mathscr{U}(\overline{\mathbf{x}}, \vartheta_r)}{\partial \vartheta} (t_{r+1} - \vartheta)^{-\gamma_1} d\vartheta.$$

The term $\frac{\partial \mathscr{U}(\overline{\mathbf{x}}, \vartheta_r)}{\partial \vartheta}$ can be approximated as

$$\frac{\partial \mathscr{U}(\overline{\mathbf{x}}, \vartheta_r)}{\partial \vartheta} = \frac{\mathscr{U}(\overline{\mathbf{x}}, \vartheta_{r+1}) - \mathscr{U}(\overline{\mathbf{x}}, \vartheta_r)}{\vartheta} + \mathcal{O}(\Delta\tau).$$

Then

$$\frac{\partial^{\gamma_1} \mathscr{U}(\overline{\mathbf{x}}, t_{q+1})}{\partial \vartheta^{\gamma_1}} \approx \frac{1}{\Gamma(1-\gamma_1)} \sum_{r=0}^{q} \frac{\mathscr{U}(\overline{\mathbf{x}}, t_{r+1}) - \mathscr{U}(\overline{\mathbf{x}}, t_r)}{\Delta\tau} \int_{r\Delta\tau}^{(r+1)\Delta\tau} (t_{r+1} - \vartheta)^{-\gamma_1} d\vartheta,$$

$$= \frac{1}{\Gamma(1-\gamma_1)} \sum_{r=0}^{q} \frac{\mathscr{U}(\overline{\mathbf{x}}, t_{q+1-r}) - \mathscr{U}(\overline{\mathbf{x}}, t_{q-r})}{\Delta\tau} \int_{r\Delta\tau}^{(r+1)\Delta\tau} (t_{r+1} - \vartheta)^{-\gamma_1} d\vartheta,$$

$$= \begin{cases} \frac{\Delta\tau^{-\gamma_1}}{\Gamma(2-\gamma_1)}(\mathscr{U}^{q+1} - \mathscr{U}^q) + \frac{\Delta\tau^{-\gamma_1}}{\Gamma(2-\gamma_1)} \sum_{r=1}^{q}(\mathscr{U}^{q+1-r} - \mathscr{U}^{q-r})\left[(r+1)^{1-\gamma_1} - r^{1-\gamma_1}\right], & q \geqslant 1 \\ \frac{\Delta\tau^{-\gamma_1}}{\Gamma(2-\gamma_1)}(\mathscr{U}^1 - \mathscr{U}^0). & q = 0, \end{cases}$$

Letting $a_0 = \frac{\Delta\tau^{-\gamma_1}}{\Gamma(2-\gamma_1)}$ and $b_r = (r+1)^{1-\gamma_1} - r^{1-\gamma_1}$, $r = 0, 1, \ldots, q$, we have

Table 1
Problem 1, results of the local meshless technique.

		N = 8		N = 10		N = 12	
	$\Delta\tau$	Max(error)	RMS	Max(error)	RMS	Max(error)	RMS
Two-term	0.1	2.8416e−04	8.8737e−05	2.9285e−04	9.2558e−05	2.9732e−04	9.5131e−05
	0.05	7.0957e−05	2.2159e−05	7.3125e−05	2.3112e−05	7.4237e−05	2.3753e−05
	0.01	2.8334e−06	8.8481e−07	2.9195e−06	9.2271e−07	2.9633e−06	9.4813e−07
	0.005	7.0756e−07	2.2096e−07	7.2896e−07	2.3039e−07	7.3980e−07	2.3671e−07
	0.001	2.8171e−08	8.7973e−09	2.9007e−08	9.1677e−09	2.9420e−08	9.4132e−09
	0.0005	7.0184e−09	2.1916e−09	7.2236e−09	2.2830e−09	7.3231e−09	2.3430e−09
Three−term	0.1	2.8404e−04	8.8701e−05	2.9272e−04	9.2515e−05	2.9716e−04	9.5082e−05
	0.05	7.0915e−05	2.2146e−05	7.3078e−05	2.3097e−05	7.4183e−05	2.3736e−05
	0.01	2.8296e−06	8.8364e−07	2.9152e−06	9.2135e−07	2.9584e−06	9.4657e−07
	0.005	7.0624e−07	2.2054e−07	7.2744e−07	2.2991e−07	7.3807e−07	2.3615e−07
	0.001	2.8053e−08	8.7602e−09	2.8870e−08	9.1244e−09	2.9266e−08	9.3636e−09
	0.0005	6.9765e−09	2.1785e−09	7.1754e−09	2.2677e−09	7.2683e−09	2.3254e−09

Table 2
Problem 1, results of the local meshless technique using N = 10.

		t = 1		t = 2		t = 3	
	γ	Max(error)	RMS	Max(error)	RMS	Max(error)	RMS
Two-term	0.2	7.3170e−07	2.3126e−07	5.3832e−07	1.7014e−07	2.9704e−07	9.3882e−08
	0.4	7.3053e−07	2.3089e−07	5.3746e−07	1.6987e−07	2.9657e−07	9.3733e−08
	0.6	7.2584e−07	2.2940e−07	5.3402e−07	1.6878e−07	2.9468e−07	9.3134e−08
	0.8	7.0765e−07	2.2364e−07	5.2065e−07	1.6455e−07	2.8731e−07	9.0801e−08
Three−term	0.2	7.3154e−07	2.3121e−07	5.3818e−07	1.7010e−07	2.9696e−07	9.3856e−08
	0.4	7.2979e−07	2.3065e−07	5.3690e−07	1.6969e−07	2.9626e−07	9.3634e−08
	0.6	7.2276e−07	2.2843e−07	5.3174e−07	1.6805e−07	2.9342e−07	9.2735e−08
	0.8	6.9547e−07	2.1979e−07	5.1169e−07	1.6171e−07	2.8237e−07	8.9235e−08
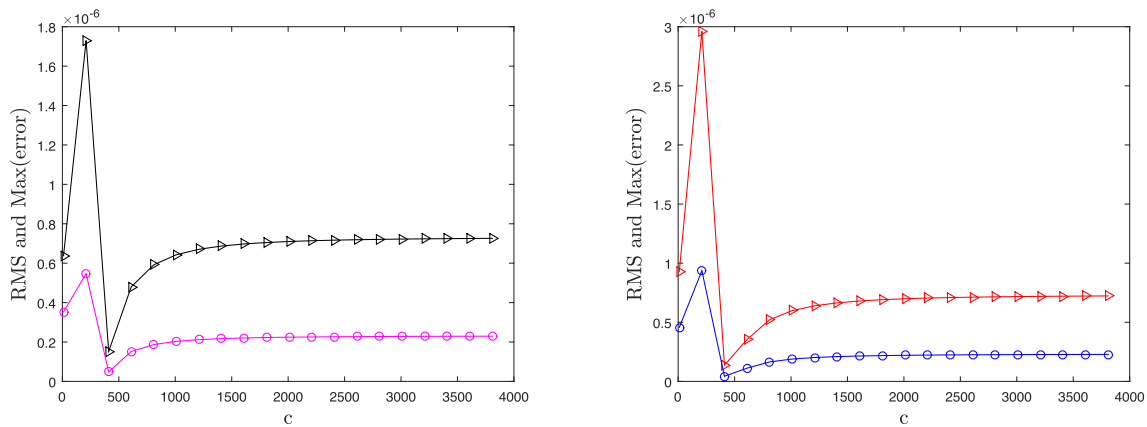
Fig. 1. Problem 1, c versus error norms (left) two-term model equation, (right) three-term model equation.

$$\frac{\partial^{\gamma_1}\mathcal{U}(\overline{\mathbf{x}}, t_{q+1})}{\partial t^{\gamma_1}} \approx \begin{cases} a_0\left(\mathcal{U}^{q+1} - \mathcal{U}^q\right) + a_0 \sum_{r=1}^{q} b_r\left(\mathcal{U}^{q+1-r} - \mathcal{U}^{q-r}\right), & q \geqslant 1 \\ a_0\left(\mathcal{U}^1 - \mathcal{U}^0\right), & q = 0. \end{cases}$$

$$(10)$$

The fractional derivative of order γ_2 and γ_3 can be found as above.

3. Results

The local meshless technique is tested for applicability, accuracy and efficiency to approximate the solution of model Eqs. (1), (2). In this paper, different computational domains are utilized with uniform and scatted nodes. Throughout the paper, we have employed the Crank-Nicolson scheme, IMQ RBF with $c = 100$, $\Delta\tau = 0.005$, and spatial domain $[0, 1]$ unless specifically stated. The accuracy is measure as follows

$$Absolute - error = |\widehat{\mathbb{U}} - \mathcal{U}|,$$
$$Max(errer) = \max(Absolute - error),$$

$$RMS = \sqrt{\frac{\sum_{h=1}^{N^n}\left(\widehat{\mathbb{U}}_h - \mathcal{U}_h\right)^2}{N}},$$

$$(11)$$

where $\widehat{\mathbb{U}}$ is the exact solution.
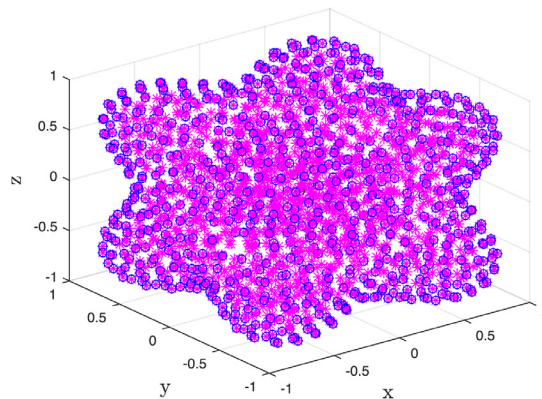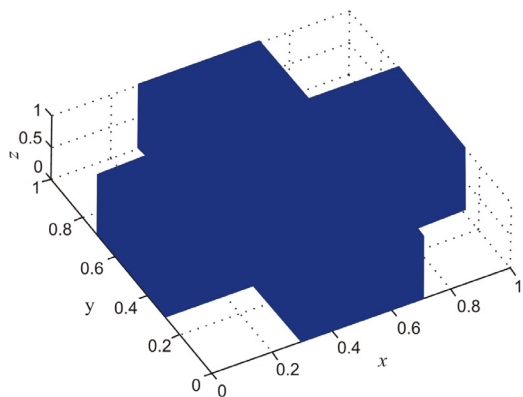
Fig. 2. *Domain-1* (left) and *Domain-2* (right).
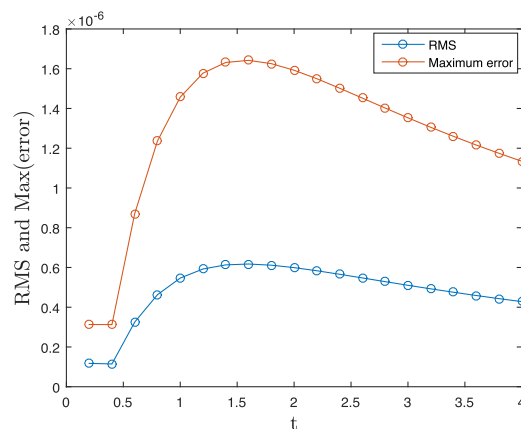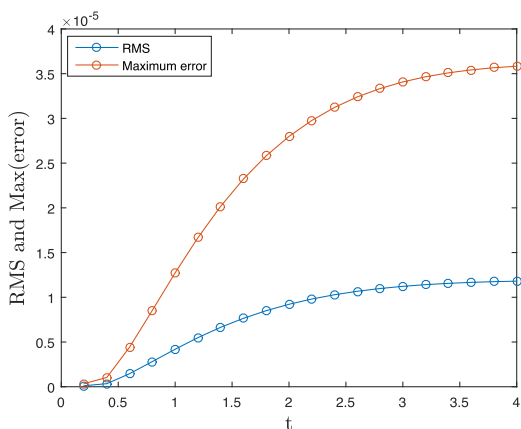
Fig. 3. Problem 1, error profile of two-term model equation (left) *Domain-1* (right) *Domain-2*.
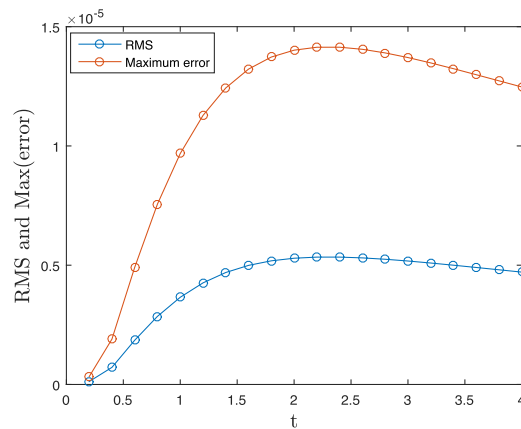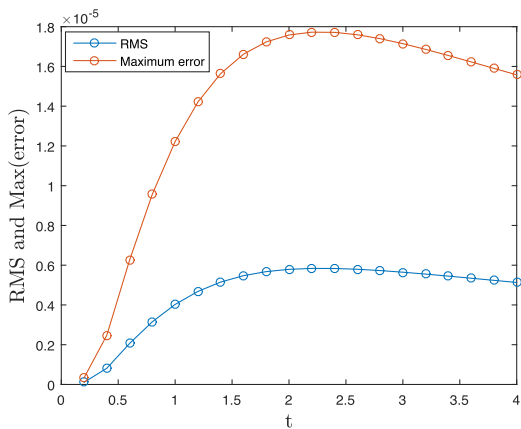
Fig. 4. Problem 1, error profile of three-term model equation (left) *Domain-1* (right) *Domain-2*.

Problem 1. The exact solution for Eqs. 1,2 with $\beta = 1, \gamma = \delta = 0$ is

$$\mathscr{U}(\overline{\mathbf{x}}, t) = e^{-t} \sin(\pi x) \sin(\pi y) \sin(\pi z), \ \overline{\mathbf{x}} \in \Omega, \tag{12}$$

The results of the proposed local meshless technique for Problem 1 are displayed in Table 1. Various number of nodes N, final time $t = 1$ and time step size $\Delta \tau$ are utilized whereas in two- and three-term time fractional model the values of fractional order are $\gamma_1 = \gamma_2 = 0.5$ and $\gamma_1 = \gamma_2 = \gamma_3 = 0.5$ respectively.

Furthermore, the error norms stand for *Max(error)* and *RMS*. These results exposed the evidence that the proposed technique is competent for better results and the accuracy increases somewhat when $\Delta \tau$ decreases. To examine the performance of the method, the results are calculated for different time fractional order γ's and final time up to $t = 3$, and shown in Table 2. Better accuracy has been obtained for various fractional order utilizing $N = 10$.

The accuracy and stability of the RBF-based meshless technique are extremely dependent on the value of the shape-parameter c, and the results will be different and unstable as the shape-parameter value changes a little. However, the accuracy and stability of the proposed technique are tested against Problem 1, as shown in Fig. 1 for $N = 10, \gamma_1 = \gamma_2 = 0.5$ (in two-term), $\gamma_1 = \gamma_2 = \gamma_3 = 0.5$ (in three-term) and $t = 1$. Fig. 1 exposed that the proposed technique is accurate and stable. In the current paper, we have studied two irregular domains which are illustrated in Fig. 2. In Figs. 3 and 4, the results are shown for Problem 1 regarding the non-rectangular domains. For two-term case, we have considered the value of $\gamma_1 = \gamma_2 = 0.1$ (for *Domain-1*) and $\gamma_1 = \gamma_2 = 0.9$ (for *Domain-2*) whereas in case of three-term, $\gamma_1 = 0.8, \gamma_2 = 0.6, \gamma_3 = 0.4$ are taken into account for both *Domain-1* and *Domain-2*, for various time up to $t = 4$. These figures visualized better accuracy in both types of domains.

Problem 2. The exact solution for Eqs. (1), (2) with $\beta = 1, \gamma = \delta = 0$ is

$$\mathscr{U}(\overline{\mathbf{x}}, t) = e^{x-y-z-t} \sin(\pi x) \sin(\pi y) \sin(\pi z), \ \overline{\mathbf{x}} \in \Omega, \tag{13}$$

Determining the accuracy of the recommended technique, results of Problem 2 are compared with the exact solution for diverse $\Delta\tau$ and N using $t = 1$ for $\gamma_1 = \gamma_2 = 0.3$ (for two-term) and $\gamma_1 = \gamma_2 = \gamma_3 = 0.3$ (for three-term). These results are shown in Table 3. In this table, we can notice that the recommended method provides better results with few iterations and is become more accurate when iterations increase and both the error norms reached up to 10^{-9}. In Table 4, the results are achieved using various γ's for $N = 10$, $t = 1, 2$ and $t = 3$. Observing this table we can say that accurate results have been achieved for various time fractional orders in this problem as well.

Table 3
Problem 2, results of the local meshless technique for $t = 1$.

	$\Delta\tau$	N = 8		N = 10		N = 12	
		Max(error)	RMS	Max(error)	RMS	Max(error)	RMS
Two-term	0.1	2.1364e−04	5.9329e−05	2.0995e−04	6.1905e−05	2.1083e−04	6.3636e−05
	0.05	5.3362e−05	1.4819e−05	5.2441e−05	1.5462e−05	5.2659e−05	1.5894e−05
	0.01	2.1334e−06	5.9244e−07	2.0964e−06	6.1814e−07	2.1051e−06	6.3539e−07
	0.005	5.3324e−07	1.4808e−07	5.2401e−07	1.5451e−07	5.2616e−07	1.5881e−07
	0.001	2.1318e−08	5.9201e−09	2.0947e−08	6.1764e−09	2.1032e−08	6.3482e−09
	0.0005	5.3278e−09	1.4795e−09	5.2349e−09	1.5435e−09	5.2559e−09	1.5863e−09
Three−term	0.1	2.1360e−04	5.9319e−05	2.0991e−04	6.1894e−05	2.1079e−04	6.3623e−05
	0.05	5.3351e−05	1.4816e−05	5.2429e−05	1.5459e−05	5.2645e−05	1.5890e−05
	0.01	2.1326e−06	5.9223e−07	2.0956e−06	6.1790e−07	2.1042e−06	6.3512e−07
	0.005	5.3302e−07	1.4802e−07	5.2376e−07	1.5443e−07	5.2588e−07	1.5873e−07
	0.001	2.1303e−08	5.9159e−09	2.0931e−08	6.1715e−09	2.1014e−08	6.3426e−09
	0.0005	5.3232e−09	1.4783e−09	5.2297e−09	1.5420e−09	5.2502e−09	1.5846e−09

Table 4
Problem 2, results of the local meshless technique using $N = 10$.

	γ	t = 1		t = 2		t = 3	
		Max(ε)	RMS	Max(ε)	RMS	Max(ε)	RMS
Two-term	0.1	5.2442e−07	1.5463e−07	3.8582e−07	1.1376e−07	2.1289e−07	6.2772e−08
	0.3	5.2401e−07	1.5451e−07	3.8552e−07	1.1367e−07	2.1273e−07	6.2724e−08
	0.7	5.1568e−07	1.5205e−07	3.7941e−07	1.1187e−07	2.0936e−07	6.1733e−08
	0.9	4.9040e−07	1.4460e−07	3.6082e−07	1.0639e−07	1.9911e−07	5.8712e−08
Three−term	0.1	5.2437e−07	1.5461e−07	3.8578e−07	1.1375e−07	2.1286e−07	6.2763e−08
	0.3	5.2376e−07	1.5443e−07	3.8532e−07	1.1361e−07	2.1262e−07	6.2691e−08
	0.7	5.1127e−07	1.5075e−07	3.7615e−07	1.1091e−07	2.0757e−07	6.1204e−08
	0.9	4.7334e−07	1.3958e−07	3.4827e−07	1.0270e−07	1.9219e−07	5.6673e−08
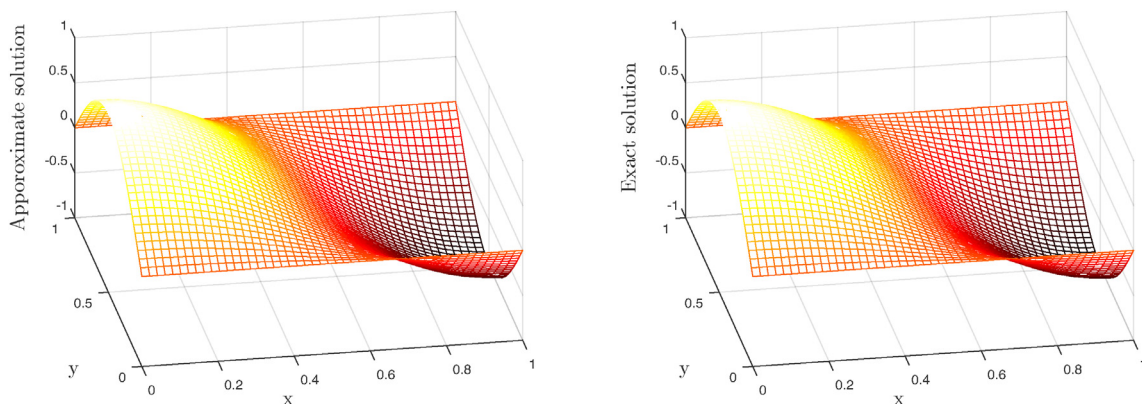
Fig. 5. Problem 3, two-term model equation at $z = 0.5$ (left) numerical solution (right) exact solution.
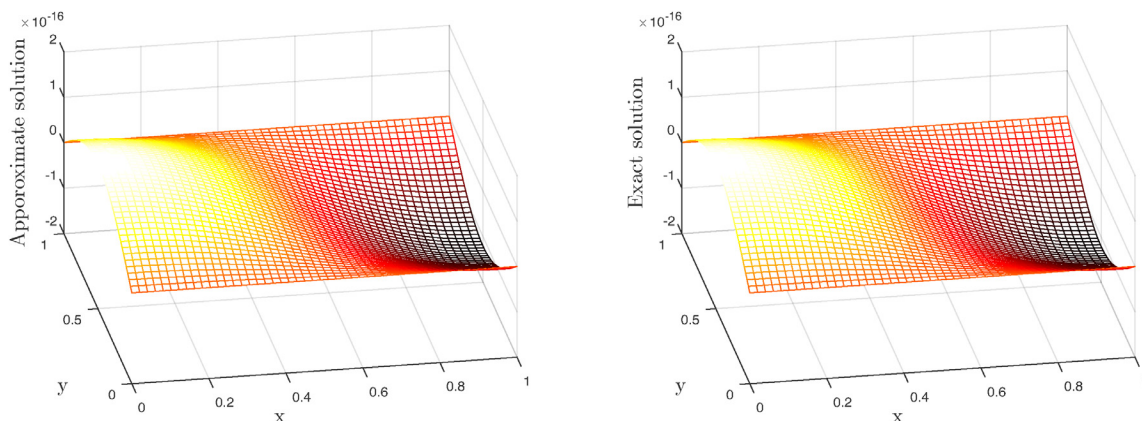
Fig. 6. Problem 3, three-term model equation at $z = 1$ (left) numerical solution (right) exact solution.

Problem 3. The exact solution for Eqs. (1), (2) with $\beta = 1$, $\gamma = 1$, $\delta = \pi^2$ is

$$\mathscr{U}(\overline{\mathbf{x}}, t) = e^t \sin(\pi x) \sin(\pi y) \sin(\pi z), \ \overline{\mathbf{x}} \in \Omega, \tag{14}$$

For Problem 3, the behavior of numerical and exact solutions using $N = 21$, $t = 0.01$ are visualized in Fig. 5 at $z = 0.5$, $\gamma_1 = \gamma_2 = 0.5$ (in two-term) whereas in Fig. 6 the solutions are shown at $z = 1$ for $\gamma_1 = \gamma_2 = \gamma_3 = 0.5$ (in three-term). One can see from these figures that the numerical solution is very compatible with the exact solution.

4. Conclusion

In this paper, we have examined the effectiveness and applicability of the suggested local meshless technique to compute the numerical solution of time fractional Sobolev model equations. The obtained results prove that the suggested technique works amazingly in fractional PDE models. Numerical experiments show that the algorithm gives good accuracy and in light of these analyses, we suggest that the local meshless technique can be implemented to such types of fractional PDE models which appear in physical problems.

Declaration of Competing Interest

The authors declare that they have no known competing financial interests or personal relationships that could have appeared to influence the work reported in this paper.

Acknowledgements

Funding

Appendix A. Supplementary data

Supplementary data associated with this article can be found, in the online version, at https://doi.org/10.1016/j.jksus.2021.101604.

References

Ahmad, I., Zaman, S., et al., 2018. Local meshless differential quadrature collocation method for time-fractional PDEs. Discrete & Continuous Dynamical Systems-S.

Ahmad, I., Siraj-ul-Islam, Khaliq, A.Q.M., 2017. Local RBF method for multi-dimensional partial differential equations. Computers & Mathematics with Applications 74, 292–324.

Ahmad, I., Riaz, M., Ayaz, M., Arif, M., Islam, S., Kumam, P., 2019a. Numerical simulation of partial differential equations via local meshless method. Symmetry 11, 257.

Ahmad, I., Ahsan, M., Hussain, I., Kumam, P., Kumam, W., 2019b. Numerical simulation of PDEs by local meshless differential quadrature collocation method. Symmetry 11 (3), 394.

Ahmad, I., Ahsan, M., Zaheer-ud-Din, M., Ahmad, P. Kumam, 2019c. An efficient local formulation for time-dependent PDEs. Mathematics 7, 216.

Ahmad, I., Ahmad, H., Thounthong, P., Chu, Y.-M., Cesarano, C., 2020a. Solution of multi-term time-fractional PDE models arising in mathematical biology and physics by local meshless method. Symmetry 12 (7), 1195.

Ahmad, H., Khan, T.A., Ahmad, I., Stanimirović, P.S., Chu, Y.-M., 2020b. A new analyzing technique for nonlinear time fractional Cauchy reaction-diffusion model equations. Results in Physics. 103462.

Ahmad, I., Khan, M.N., Inc, M., Ahmad, H., Nisar, K., 2020c. Numerical simulation of simulate an anomalous solute transport model via local meshless method. Alexandria Engineering Journal 59 (4), 2827–2838.

Ahmad, H., Seadawy, A.R., Khan, T.A., 2020d. Study on numerical solution of dispersive water wave phenomena by using a reliable modification of variational iteration algorithm. Mathematics and Computers in Simulation.

Ahmad, H., Seadawy, A.R., Khan, T.A., Thounthong, P., 2020e. Analytic approximate solutions for some nonlinear parabolic dynamical wave equations. Journal of Taibah University for Science 14 (1), 346–358.

Ahmad, H., Khan, T.A., Stanimirovic, P.S., Ahmad, I., 2020f. Modified variational iteration technique for the numerical solution of fifth order KdV type equations. J. Appl. Comput. Mech., 236–242

Ahmad, I., Ahmad, H., Inc, M., Yao, S.-W., Almohsen, B., 2020g. Application of local meshless method for the solution of two term time fractional-order multi-dimensional PDE arising in heat and mass transfer. Thermal Science 24 (Suppl. 1), 95–105.

Ahmad, I., Ahmad, H., Abouelregal, A.E., Thounthong, P., Abdel-Aty, M., 2020h. Numerical study of integer-order hyperbolic telegraph model arising in physical and related sciences. The European Physical Journal Plus 135 (9), 1–14.

Ain, Q.T., He, J.-H., 2019. On two-scale dimension and its applications. Thermal Science 23 (3 Part B), 1707–1712..

Caputo, M., 1967. Linear models of dissipation whose Q is almost frequency independent–ii. Geophysical Journal International 13 (5), 529–539.

He, J.-H., 2014. A tutorial review on fractal spacetime and fractional calculus. International Journal of Theoretical Physics 53 (11), 3698–3718.

He, J.-H., 2018. Fractal calculus and its geometrical explanation. Results in Physics 10, 272–276.

He, J.-H., Ain, Q.-T., 2020. New promises and future challenges of fractal calculus: from two-scale thermodynamics to fractal variational principle. Thermal Science (00), 65–65..

He, J.-H., El-Dib, Y.O., 2020a. Homotopy perturbation method for Fangzhu oscillator. Journal of Mathematical Chemistry 58 (10), 2245–2253.

He, J.-H., El-Dib, Y.O., 2020b. Periodic property of the time-fractional Kundu–Mukherjee–Naskar equation. Results in Physics 19, 103345.

He, J.-H., Elagan, S., Li, Z., 2012. Geometrical explanation of the fractional complex transform and derivative chain rule for fractional calculus. Physics Letters A 376 (4), 257–259.

Hussain, Z., Khan, S., Ullah, A., Ayaz, M., Ahmad, I., Mashwani, W.K., Chu, Y.-M., et al., 2020. Extension of optimal homotopy asymptotic method with use of Daftardar-Jeffery polynomials to Hirota-Satsuma coupled system of Korteweg–de Vries equations. Open Physics 18 (1), 916–924.

Inc, M., Khan, M.N., Ahmad, I., Yao, S.-W., Ahmad, H., Thounthong, P., 2020. Analysing time-fractional exotic options via efficient local meshless method. Results in Physics 103385.

Khan, M.N., Siraj-ul-Islam, Hussain, I., Ahmad, I., Ahmad, H., 2020. A local meshless method for the numerical solution of space-dependent inverse heat problems. Mathematical Methods in the Applied Sciences..

Nadeem, M., Li, F., 2019. He–Laplace method for nonlinear vibration systems and nonlinear wave equations. Journal of Low Frequency Noise, Vibration and Active Control 38 (3–4), 1060–1074.

Nawaz, R., Zada, L., Ullah, F., Ahmad, H., Ayaz, M., Ahmad, I., Nofal, T.A., 2021. An extension of optimal auxiliary function method to fractional order high dimensional equations. Alexandria Engineering Journal 60 (5), 4809–4818.

Shu, C., 2000. Differential Quadrature and Its Application in Engineering. Springer-Verlag, London.

Srivastava, M.H., Ahmad, H., Ahmad, I., Thounthong, P., Khan, N.M., 2020. Numerical simulation of three-dimensional fractional-order convection-diffusion PDEs by a local meshless method. Thermal Science, 210.

Wang, F., Zheng, K., 2016. The method of fundamental solutions for steady-state groundwater flow problems. Journal of the Chinese Institute of Engineers 39 (2), 236–242.

Wang, F., Zheng, K., Li, C., Zhang, J., 2019. Optimality of the boundary Knot method for numerical solutions of 2D Helmholtz-type equations. Wuhan University Journal of Natural Sciences 24 (4), 314–320.

Wang, F., Khan, A., Ayaz, M., Ahmad, I., Nawaz, R., Gul, N., 2020. Formation of intermetallic phases in ion implantation. Journal of Mathematics 2020.

Wang, F., Zheng, K., Ahmad, I., Ahmad, H., 2021. Gaussian radial basis functions method for linear and nonlinear convection–diffusion models in physical phenomena. Open Physics 19 (1), 69–76.